Hydrocracking of C$_5$-Isolated Asphaltene and Its Fractions in Batch and Semi-Batch Reactors

Ngoc Thuy Nguyen [ID]**, Ki Hyuk Kang** [ID]**, Pill Won Seo, Narae Kang, Duy Van Pham, Chiwoong Ahn, Gyoo Tae Kim and Sunyoung Park** *[ID]

Center for Convergent Chemical Process, Korea Research Institute of Chemical Technology (KRICT), Daejeon 34114, Korea; nnthuy@krict.re.kr (N.T.N.); khkang@krict.re.kr (K.H.K.); pwseo@krict.re.kr (P.W.S.); nkang615@krict.re.kr (N.K.); duypham@krict.re.kr (D.V.P.); ahncw@krict.re.kr (C.A.); sk6089@krict.re.kr (G.T.K.)
* Correspondence: spark517@krict.re.kr; Tel.: +82-42-860-7561

check for
updates

Abstract: Non-catalytic and catalytic hydrocracking of C$_5$-isolated asphaltene and its subfractions were performed in batch and semi-batch reactors at various temperatures. Catalyst and H$_2$ played an important role in the hydrocracking of asphaltenes. In the batch system, the catalyst enhanced asphaltene conversion to light liquid products and suppressed coke formation. The coke formation was controlled at a low reaction temperature, but the reaction rate was too low. Light liquid products were also formed at the beginning of the reaction even at high temperatures, but the coke formation was predominant as the reaction time went on due to the decrease in H$_2$ amount in the reactor. To solve these problems, H$_2$ was continuously supplied during the reaction using the semi-batch system. Sufficient supply of H$_2$ improved the conversion of asphaltenes to light liquid products while inhibiting the coke formation. The lightest asphaltene fraction was easily cracked into light products by inhibiting the coke formation, while the heaviest fraction tends to form coke. The lightest asphaltene fraction prolonged the coke induction period of the heaviest fraction during the catalytic hydrocracking because the lightest fraction contained a significant amount of heavy resin close to that which could prevent aggregation of the heaviest asphaltenes.

Keywords: slurry-phase hydrocracking; asphaltenes; vacuum residue; dispersed catalyst

1. Introduction

The slurry-phase hydrocracking of heavy oil is the process for converting residual feedstocks to lower boiling products [1,2]. The main functions of the dispersed catalyst are converting hydrogen gas into active hydrogen, suppressing coke formation, and promoting hydroconversion [3–5]. Moreover, the hydrogen pressure significantly affects the composition of hydrocracker products [6,7].

Asphaltene is the heaviest fraction in heavy oils and residues, which consists of polynuclear aromatic hydrocarbons containing alicyclic substituents and long aliphatic chains with a high content of trace metals (V and Ni) and heteroatoms (S, N, and O) [8–10]. The effect of asphaltenes on the refinery process is that asphaltene molecules lose their alkyl side chains through thermolysis, which results in the aggregation and precipitation of polyaromatic sheets into coke [11–13], causes fouling, rapid catalyst deactivation, and decrease of reaction rate [14–21]. In our previous study [22], the effect of asphaltene contents on hydrocracking of heavy feedstocks was investigated. It was noted that the increase of asphaltenes in the feedstock reduced product quality, increasing the micro carbon residue (MCR) and S, N, V, and Ni contents. Hence, the amount of coke significantly increased and the yield for liquid product decreased. Therefore, a study on asphaltene upgrading would benefit the hydrocracking processes.

Recently, several studies on the upgrading of asphaltenes based on thermal treatment were reported [23–27]. Thermal treatment leads to the dealkylation of aliphatic chains of asphaltenes and results in hydrogen depletion, carbon enrichment, and then coke formation. Generally, the coke formation rate is fast at a high reaction temperature, and the molecular weight loss of the remaining asphaltenes decreases during the pyrolysis. This is because asphaltenes are converted into maltene, gas, and coke during pyrolysis and the maltene is also then transformed into asphaltenes and coke by polymerization [23,27]. It has been reported that H_2 inhibited overcracking and the condensation of hydrocarbon free radicals, so the coke and gas formation were limited and the Conradson carbon residue (CCR) of the hydrocracking products decreased [6,7]. It has been also reported that the conversion of residue as well as sulfur in the semi-batch reactor was higher than the batch system [28].

Previous studies mainly contributed to the understanding of asphaltenes behavior during the thermal treatment. However, there is a lack of knowledge on the role of slurry-phase catalysts and H_2 pressure on the hydrocracking of asphaltenes. Moreover, examining the effect of reaction temperature on hydrocracking of asphaltenes would add value. The contribution of catalysts on reducing coke formation and increasing liquid yield during heavy oil upgrading containing maltene and asphaltenes was investigated in previous studies [22,29–33], but the coke suppression by the catalysts was not explained in detail. It was known that asphaltenes could be fractionated using a binary solvent system such as toluene–heptane or methylene chloride–pentane to characterize the properties of the fractions and compare them to the unfractionated asphaltenes [34,35]. The differences in properties between the fractionated and unfractionated asphaltenes were only highlighted. Therefore, study on the hydrocracking of fractionated asphaltenes is needed to confirm more detailed hydrocracking properties of asphaltenes.

The objective of this study was to elucidate the effect of Mo-octoate catalyst precursor, reaction temperature, and H_2 pressure on non-catalytic and catalytic hydrocracking of C_5-asphaltene (C_5-Asp) by comparing yield for coke, H_2 consumption, and saturates, aromatics, resins, and asphaltenes (SARA) distribution of deasphalted oil (DAO) products obtained in semi-batch and batch systems. The study aim was to improve the understanding of the role of slurry-phase catalyst, H_2 pressure, and reaction temperature on the conversion of asphaltenes into coke. Moreover, semi-batch catalytic hydrocracking of asphaltene subfractions obtained from a C_5-Asp feedstock was conducted to determine the reaction tendency of each fraction as well as to identify the main coke precursor.

2. Materials and Methods

2.1. Materials

The C_5-Asp feedstock was precipitated from a vacuum residue following the ASTM D-3279 method using n-pentane as a solvent. The detailed procedure to separate the C_5-Asp feedstock was described in our previous study [36]. The C_5-Asp was fractionated into three fractions by Soxhlet extraction using n-hexane and tetrahydrofuran (THF). Figure 1 shows the procedure for obtaining the asphaltene fractions. A certain amount of C_5-Asp and binary solvent 1 (80 wt.% n-hexane and 20 wt.% THF) were mixed with a ratio of solvent/C_5-Asp of 60. The mixture was filtered to obtain precipitate 1 and filtrate 1. Soxhlet extraction was used to remove the remaining filtrate 1 from precipitate 1. The lightest asphaltene fraction (C_5-Asp-1) was recovered from filtrate 1 using a rotary evaporator. For the subsequent separation, C_5-Asp-2 was obtained from the precipitate 1 (the residue of C_5-Asp after removing C_5-Asp-1) following a similar procedure using solvent 2 (70 wt.% n-hexane and 30 wt.% THF). C_5-Asp-3, the heaviest asphaltene fraction, was obtained as the remaining solid after drying precipitate 2. The properties of the C_5-Asp and the fractions are summarized in Table 1.

The solvents such as toluene, *n*-pentane, *n*-hexane, and THF were purchased from SAMCHUN Chemical, Korea. The catalyst precursor used in this study was Mo-octoate with 15.4 wt.% of Mo obtained from Shepherd Chemical, United States.
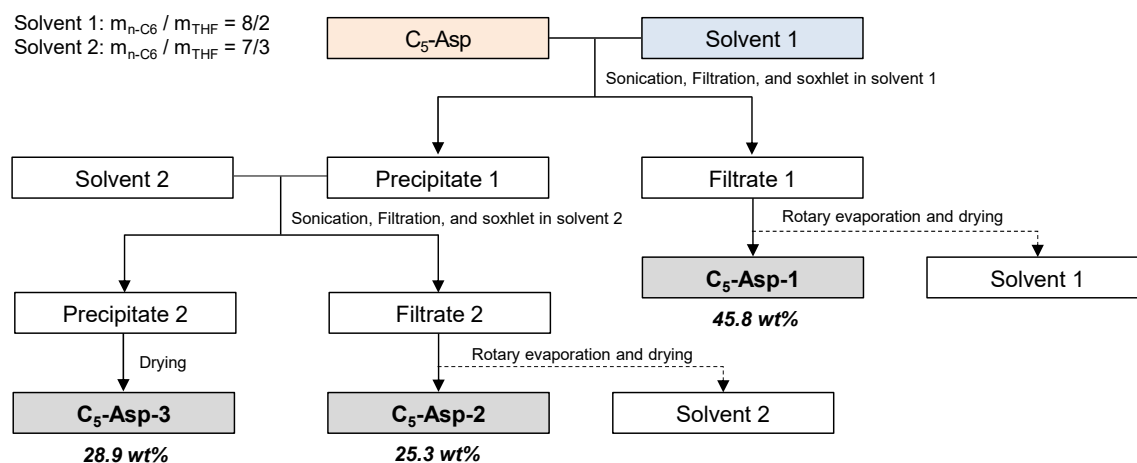
Solvent 1: m_{n-C6} / m_{THF} = 8/2
Solvent 2: m_{n-C6} / m_{THF} = 7/3

Figure 1. The procedure for fractionation of C_5-Asp.

Table 1. Properties of C_5-Asp feedstock and its subfractions.

Properties	C_5-Asp	C_5-Asp-1	C_5-Asp-2	C_5-Asp-3
C (wt.%)	82.1	81.4	81.6	81.5
H (wt.%)	8.1	8.5	7.8	7.4
N (wt.%)	1.0	0.8	1.1	1.2
S (wt.%)	7.2	6.7	7.4	7.9
H/C atomic ratio	1.18	1.25	1.15	1.09
Ni (wppm)	170	100	210	280
V (wppm)	810	480	990	1300
MCR (wt.%)	48.3	39.6	51.4	57.6

2.2. Experimental Section

Non-catalytic and catalytic hydrocracking of C_5-Asp and its fractions were conducted in semi-batch and batch 100 mL reactors, using 1000 wppm of Mo from Mo-octoate in the catalytic reaction. In the batch reactor, non-catalytic and catalytic hydrocracking reactions were conducted as reported in our previous study [36]. During the hydrocracking reaction, the reaction pressure decreased due to the H_2 consumption. In semi-batch hydrocracking, H_2 was supplied continuously into the reactor to maintain the reaction pressure, which was kept constant by a regulator at 110 bar. The volume of H_2 added at the initial condition (80 bar at 80 °C) and during the reaction was recorded to calculate the H_2 consumption. After the reactions, products were fractionated into coke, residual asphaltenes, DAO, and gas. The yields for products were calculated and the percentage of sulfur removal (H_2S in the gas phase) was also determined by the equation below:

$$\text{S removal (\%)} = 100 - 100 \times (S_{Asp} + S_{DAO} + S_{coke})/S_{feedstock},$$

where S removal is the percentage of sulfur present in the gas phase, $S_{feedstock}$, S_{Asp}, S_{DAO}, and S_{coke} are the percentages of sulfur determined by EA analysis in the asphaltene feedstocks, residual asphaltenes, DAO, and coke, respectively.

2.3. Characterization of Products

The remaining H_2 after the hydrocracking reaction was determined by a YL6500 GC (Young Lin instrument, Korea) with a TCD detector to calculate the amount of H_2 consumed. SARA in DAO products were identified using SARA instrument with a Chromarod-S5 column (IATROSCAN MK-6s, Mitsubishi, Japan). Inductively coupled plasma-atomic emission spectrometer (iCAP 7400 ICP-OES, Thermo Scientific, USA) was used to examine the V and Ni contents. To determine the C, H, N, and S contents, elemental analyzer (Flash EA-2000, Thermo Scientific, USA) was used. The MCR was identified

by a micro carbon residue tester (MCRT-160, PAC, USA). XRD instrument (Ultima IV diffractometer, Rigaku, Japan) with Cu-Kα radiation (λ = 1.5418 Å) of 40 kV and 40 mA was used to investigate the coke structure. Thermogravimetric analysis (SDT Q600, TA instruments, USA) was conducted a heating rate 5 °C/min and a temperature range of 30–800 °C under a constant air flow of 100 mL/min.

3. Results and Discussion

3.1. Non-Catalytic and Catalytic Hydrocracking of C$_5$-Asp in the Batch Reactor

Figure 2 shows the effect of reaction temperature (380, 410, and 430 °C) and catalyst on yields for gas, coke, and DAO obtained from the non-catalytic and catalytic hydrocracking of C$_5$-Asp in the batch reactor. During the non-catalytic hydrocracking at 410 and 430 °C, the yield for DAO decreased as the reaction time went on (Figure 2e,f). The reduction in DAO yield was greater than the increase in gas yield, indicating that the DAO was cracked into gas products and also converted into heavier fractions such as asphaltenes and coke. This result is similar with the previous study suggesting that the maltene content decreased as the reaction temperature increased from 400 to 450 °C through gas, coke, and asphaltene formation [27]. It is noted that the conversion of DAO and asphaltenes to heavier fractions at a higher reaction temperature was faster, resulting in a rapid increase in coke formation. The higher the reaction temperature, the higher the coke formation rate, resulting in a steep slope of the curve shown in Figure 2. This tendency of coke formation obtained during the non-catalytic hydrocracking at high reaction temperatures is consistent with previous reports related to asphaltene pyrolysis at various reaction temperatures and times [23,24].
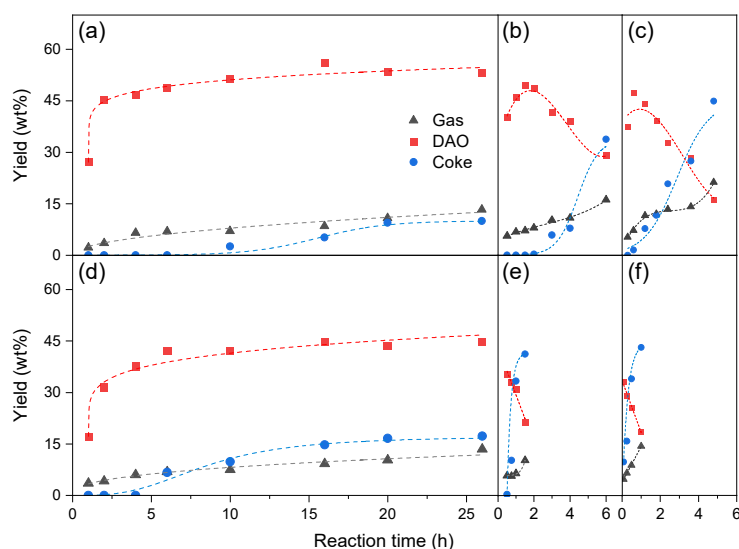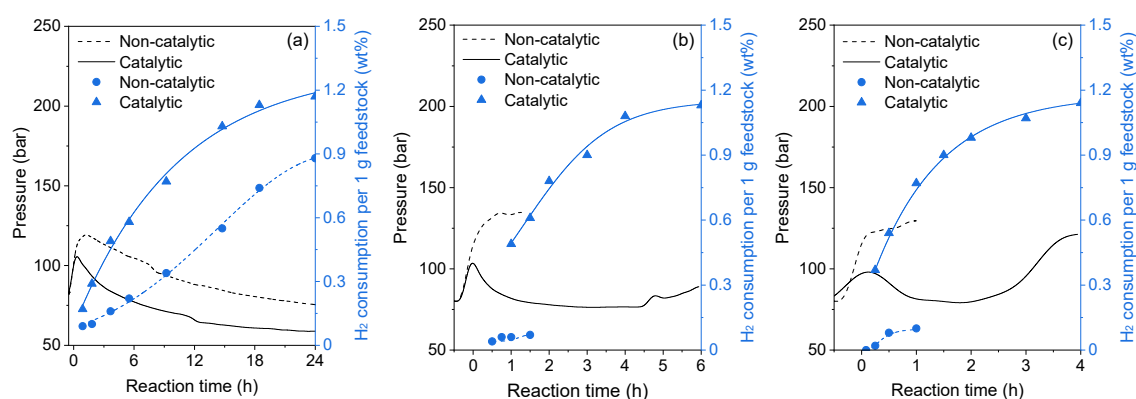

Figure 2. Yields for gas, deasphalted oil (DAO), and coke in catalytic hydrocracking of C5-Asp at (**a**) 380, (**b**) 410, and (**c**) 430 °C and non-catalytic hydrocracking of C$_5$-Asp at (**d**) 380, (**e**) 410, and (**f**) 430 °C. Reaction conditions: batch reactor, P$_{H2}$ = 80 bar at 80 °C, and 1000 wppm of Mo from Mo-octoate in catalytic hydrocracking.

Figure 2b,c shows that the DAO yield in the catalytic hydrocracking increased to a maximum value and then decreased as the reaction time went on. The maximum DAO yield depended on the reaction temperature, and a higher maximum DAO yield was obtained at low temperature. The presence of catalyst prolonged the coke induction periods. Moreover, the coke formation rate obtained from the catalytic hydrocracking was much lower than that obtained from the non-catalytic hydrocracking reaction. This result indicates that C$_5$-Asp could initially be converted to lighter products during the catalytic hydrocracking in the batch system, and thereafter the significant increase in coke formation was due to the decrease of H$_2$ amount in the batch reactor.

The product distribution at 380 °C was also shown in Figure 2a,d. The yields for DAO and coke at this condition were totally different to those obtained at higher reaction temperatures. The yield for DAO increased, then remained constant without decrease, and the rate of coke formation was much slower than the higher temperature results. This implies that the conversion of DAO into heavier fractions does not occur at 380 °C. It has been reported that the hydrogenation reaction dominated in the hydrocracking of heavy oil at 380 °C [14,37,38]. These are well correlated to the fact that a significant amount of H_2 was consumed and the coke formation was suppressed effectively at 380 °C.

Figure 3 shows the pressure profile and H_2 consumption obtained from non-catalytic and catalytic hydrocracking of C_5-Asp in the batch reactor. During the non-catalytic hydrocracking at 410 and 430 °C, almost no H_2 was consumed and the reaction pressure increased due to the gas formation, while the H_2 consumption increased significantly and the reaction pressure decreased continuously at 380 °C even without the catalyst. The catalyst improved the H_2 consumption and decreased the reaction pressure at the beginning of the reaction. The reaction pressure then increased at 410 and 430 °C as shown in Figure 3b,c. However, it was observed that the reaction pressure decreased continuously because the hydrogenation reaction dominated at 380 °C. These results are consistent with Figure 2. The catalyst improved the DAO yield and reduced the coke yield. The increase in DAO yield and the decrease in coke yield were related to the increase in H_2 consumption because the catalyst improved the hydrogenation reactions and stabilized the radicals to reduce the coke formation.


Figure 3. The profiles of reaction pressure and H_2 consumption per 1 g feedstock obtained from non-catalytic and catalytic hydrocracking of C_5-Asp in batch reactor at (**a**) 380, (**b**) 410, and (**c**) 430 °C. Reaction conditions: batch reactor, P_{H2} = 80 bar at 80 °C, and 1000 wppm of Mo from Mo-octoate in catalytic hydrocracking.

Figure 4 exhibits the effect of reaction temperature and catalyst on yields for resins, aromatics, and saturates in the liquid product by non-catalytic and catalytic hydrocracking of C_5-Asp in the batch reactor. Figure 4a,d shows that the conversion of asphaltenes to aromatics was preferred during the hydrocracking of C_5-Asp at 380 °C, whereas yields for aromatics and resins decreased during the hydrocracking at 410 and 430 °C even though the catalyst was used. Yields for aromatics and resins showed the maximum values and then decreased during the catalytic hydrocracking at 410 and 430 °C, because H_2 amount in the batch reactor decreased as the reaction time went on and coke formation was then predominant.

Summarizing the catalyst performance in the batch reactor, the addition of catalyst increased the asphaltene conversion into light liquid products and suppressed the coke formation. It seemed that the hydrocracking of C_5-Asp in the batch reactor should be conducted at a low reaction temperature of 380 °C to suppress the coke formation, but the reaction rate was too low. It was also observed that light liquid products were formed from asphaltenes at the beginning of the hydrocracking reaction even at high temperatures, but the coke formation was then predominant as the reaction time went on due to the decrease in H_2 amount in the reactor. To solve these problems, a semi-batch system was

introduced, and H_2 was continuously supplied during the reaction. The role of H_2 in the catalytic hydrocracking of C_5-Asp was examined from the results obtained from batch and semi-batch systems.
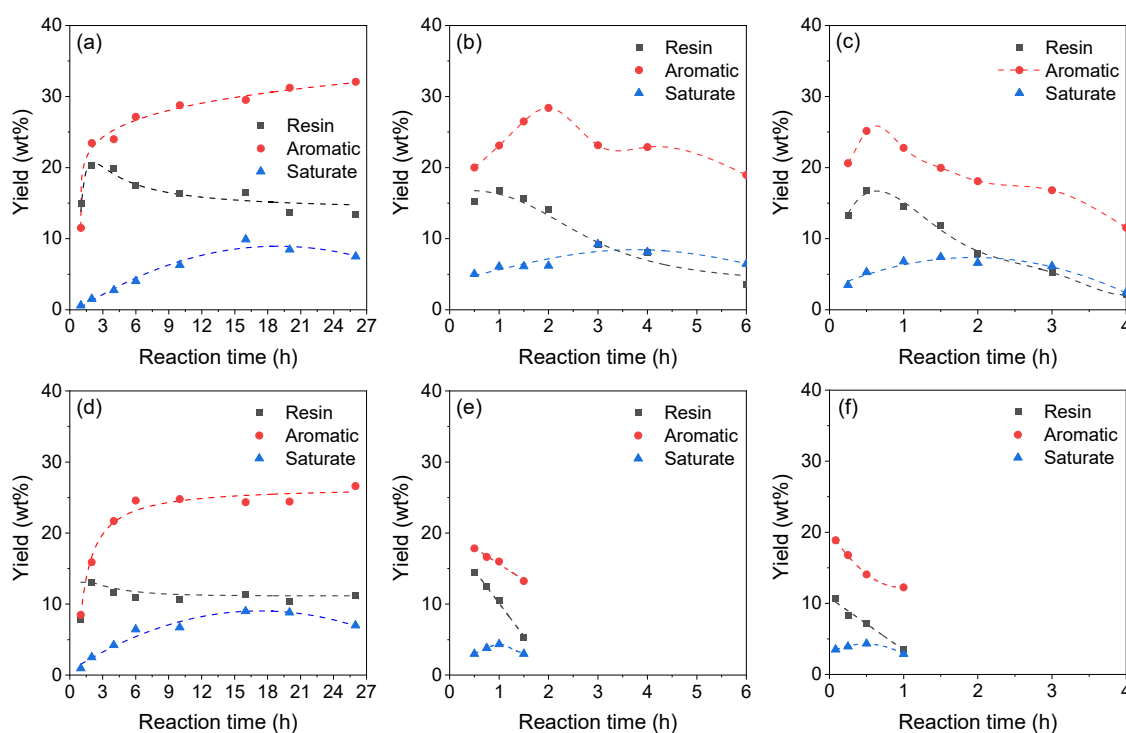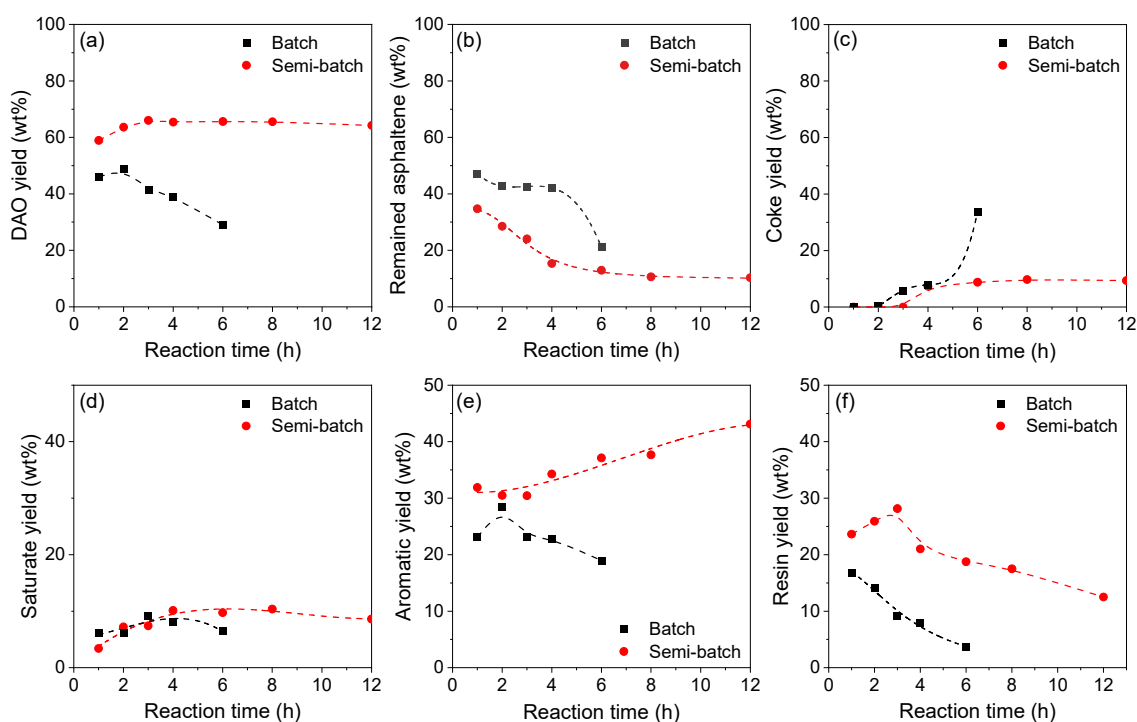

Figure 4. Yields for resins, aromatics, and saturates in catalytic hydrocracking of C5-Asp at (**a**) 380, (**b**) 410, and (**c**) 430 °C and non-catalytic hydrocracking of C_5-Asp at (**d**) 380, (**e**) 410, and (**f**) 430 °C. Reaction conditions: batch reactor, P_{H2} = 80 bar at 80 °C, and 1000 wppm of Mo from Mo-octoate in catalytic hydrocracking.

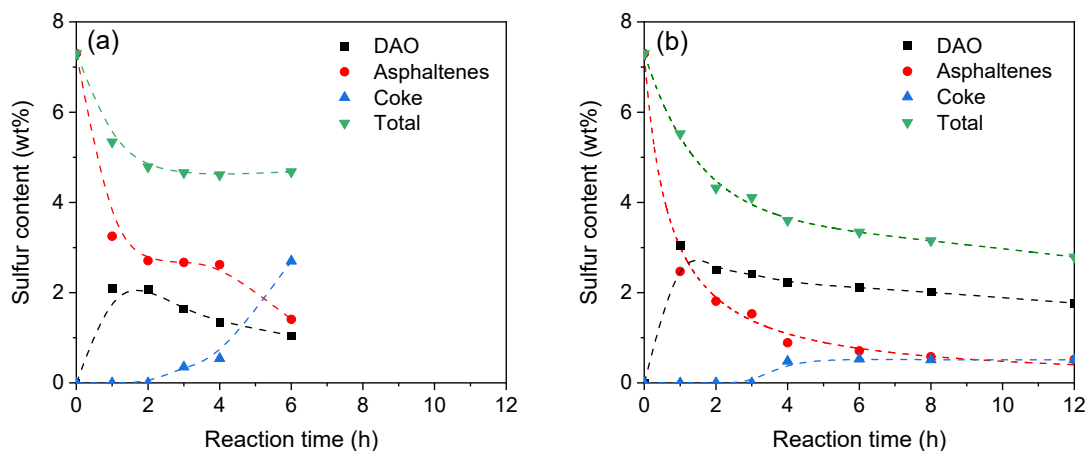### 3.2. Hydrocracking of C_5-Asp in the Semi-Batch Reactor at 410 °C

Figure 5 shows the yields for DAO, remaining asphaltenes, and coke as well as the SARA fraction of DAO obtained from the catalytic hydrocracking of C_5-Asp at 410 °C in the batch and semi-batch reactors. Yield for DAO decreased and yield for coke increased as the reaction time went on because of the limited H_2 consumption in the batch reactor, as shown in Figure 3b. On the contrary, yield for DAO obtained from the semi-batch system increased and remained almost constant. Yield for coke also increased and remained almost constant during the catalytic hydrocracking of C_5-Asp in the semi-batch reactor. Moreover, coke induction period was prolonged in the semi-batch system. These indicate that the coke formation can be controlled by maintaining high H_2 pressure in the semi-batch system. These observations also correspond to increase in H_2 consumption per gram of feedstock from 2.1 to 6.5 wt.% at reaction times of 1–12 h. Sufficient supply of H_2 during the catalytic hydrocracking of asphaltenes in the semi-batch system improved the conversion of asphaltenes to resins and aromatics while inhibiting the coke formation.

Sulfur content of DAO, remaining asphaltenes, and coke obtained from the catalytic hydrocracking of C_5-Asp was investigated to determine the effect of H_2 on the removal of sulfur (converting to gaseous product). As shown in Figure 6, total sulfur content was calculated from each sulfur content of DAO, remaining asphaltenes, and coke. It was observed that the total sulfur content was similarly reduced in batch and semi-batch reactors during the first 2 h. However, the total sulfur content was more significantly changed after longer reaction time. The total sulfur content was almost constant in the batch reactor, while it decreased in the semi-batch reactor. It seemed that sulfur just moved from asphaltenes to coke without removal in the batch system. This was related to the observation that DAO and asphaltenes were condensed to coke after 2 h catalytic hydrocracking reaction in the batch system

as shown in Figure 2. In contrast, the sulfur content of DAO and remaining asphaltenes obtained from the catalytic hydrocracking in the semi-batch system steadily decreased while maintaining the sulfur content of coke constant as the reaction time went on. These results indicate that sufficient H_2 supply during the catalytic hydrocracking of asphaltenes facilitates hydrodesulfurization (HDS) reaction with H_2S production. It has been reported that ring opening improved during the hydrocracking reaction in the semi-batch reactor, facilitating the removal of sulfur located inside the rings [39,40]. It was also observed that HDS of coke was unlikely to occur during the hydrocracking reaction. This implies that once the coke is formed, the sulfur-containing polyaromatic rings hardly crack.

Figure 5. Yields for (**a**) DAO, (**b**) remaining asphaltenes, (**c**) coke, (**d**) saturates, (**e**) aromatics, and (**f**) resins in catalytic hydrocracking of C_5-Asp using a batch and semi-batch system. Reaction conditions: T = 410 °C, P_{H2} = 80 bar at 80 °C (batch) or 110 bar at 410 °C (semi-batch), and 1000 wppm of Mo from Mo-octoate in catalytic hydrocracking.

Figure 6. Sulfur content of DAO, remaining asphaltenes, coke, and total content after the catalytic hydrocracking of C_5-Asp in (**a**) a batch and (**b**) semi-batch system. Reaction conditions: T = 410 °C, P_{H2} = 80 bar at 80 °C (batch) or 110 bar at 410 °C (semi-batch), and 1000 wppm of Mo from Mo-octoate in catalytic hydrocracking.

3.3. Catalytic Hydrocracking of Asphaltene Subfractions in the Semi-Batch Reactor at 410 °C

It has been reported that fractionated asphaltenes exhibited quite different properties to the unfractionated asphaltenes and asphaltenes quality was more important than the quantity in the coke formation [34,41]. Therefore, it was expected that different product distributions could be obtained from the catalytic hydrocracking of each asphaltene subfraction. In this work, C_5-Asp was separated into three fractions, which were applied to the catalytic hydrocracking reactions to understand the detailed reaction schemes of asphaltenes. Basic properties of C_5-Asp and asphaltene subfractions (C_5-Asp-1, C_5-Asp-2, and C_5-Asp-3) are summarized in Table 1. It was observed that high polar solvents produced heavier asphaltene fractions with large amounts of hetero-atom and MCR, and low H/C ratio. It was also observed that the most insoluble fraction (C_5-Asp-3) contained the highest content of metals, S, and N, resulting in a more complex structure [34].

Figure 7 shows the yields for DAO, remaining asphaltenes, and coke as well as H_2 consumption and sulfur removal obtained from the catalytic hydrocracking of asphaltene subfractions in the semi-batch system. The most soluble asphaltene faction (C_5-Asp-1) showed a higher yield for DAO and a lower yield for coke than C_5-Asp-2 and C_5-Asp-3. Moreover, the amount of remaining asphaltenes obtained from the catalytic hydrocracking of C_5-Asp-1 was lowest in all the reaction times, especially 85% of asphaltenes was converted during the first hour of the reaction. This implies that the most soluble asphaltene fraction was easily cracked into light products by inhibiting the coke formation during the catalytic hydrocracking. It was observed that the amount of remaining asphaltenes obtained from the catalytic hydrocracking of C_5-Asp-2 was slightly higher than that obtained from C_5-Asp-3 because the most insoluble asphaltene fraction could convert rapidly to the coke. It was also observed that the coke induction period was affected by the asphaltenes quality. The most insoluble fraction (C_5-Asp-3) exhibited the shortest coke induction period, observing that a lot of coke was already formed at the beginning of the reaction. From the comparison of Figures 6b and 7c, it can be inferred that the most soluble fraction (C_5-Asp-1) inhibited the conversion of C_5-Asp-3 to the coke because the C_5-Asp-1 contained a considerable amount of heavy resin, which can prevent the aggregation of C_5-Asp-3 molecules. C_5-Asp-1 showed a lower H_2 consumption than C_5-Asp-2 and C_5-Asp-3 since C_5-Asp-2 and C_5-Asp-3 exhibited higher aromaticity. However, less H_2 was consumed during the catalytic hydrocracking of C_5-Asp-3 than that of C_5-Asp-2 because C_5-Asp-3 molecules rapidly aggregated to form the coke due to the limit of catalyst activity. It was also observed that the sulfur removal to H_2S (HDS) was similar for the asphaltene fractions although the sulfur content in each asphaltene fraction was different.

3.4. Properties of Coke Produced from Catalytic Hydrocracking of Asphaltene Subfractions

It is known that catalyst deactivation is caused by formation of coke and properties of the coke also affect the deactivation [42]. It has been also reported that hard graphitic coke caused mainly catalyst deactivation [43]. The slurry-phase Mo catalyst particles encapsulated by hard graphitic coke were deactivated and no longer participated in the hydroconversion reaction. Therefore, the change of properties of the coke obtained from the catalytic hydrocracking of asphaltene subfractions was examined to understand the catalyst deactivation caused by each fraction in this work.

Before analyzing the coke, ICP analysis was performed to check the position of Mo catalyst after the catalytic hydrocracking of asphaltene subfractions. It was observed that all the Mo metal determined was contained in the coke, which was consistent with the previous report [28]. Figure 8 shows the H/C atomic ratio of coke obtained from the catalytic hydrocracking of asphaltene subfractions in the semi-batch system. Obviously, H/C atomic ratio of coke decreased as the reaction time went on, implying that the coke became more carbonaceous due to the cracking reaction. H/C atomic ratio is considered as one of the parameters to determine the condensation degree of hydrocarbon compounds. The H/C atomic ratio of coke decreased in the following order: C_5-Asp-1 > C_5-Asp-2 > C_5-Asp-3. This indicates that the more carbonaceous and condensed coke was formed from the heavier asphaltene subfractions.
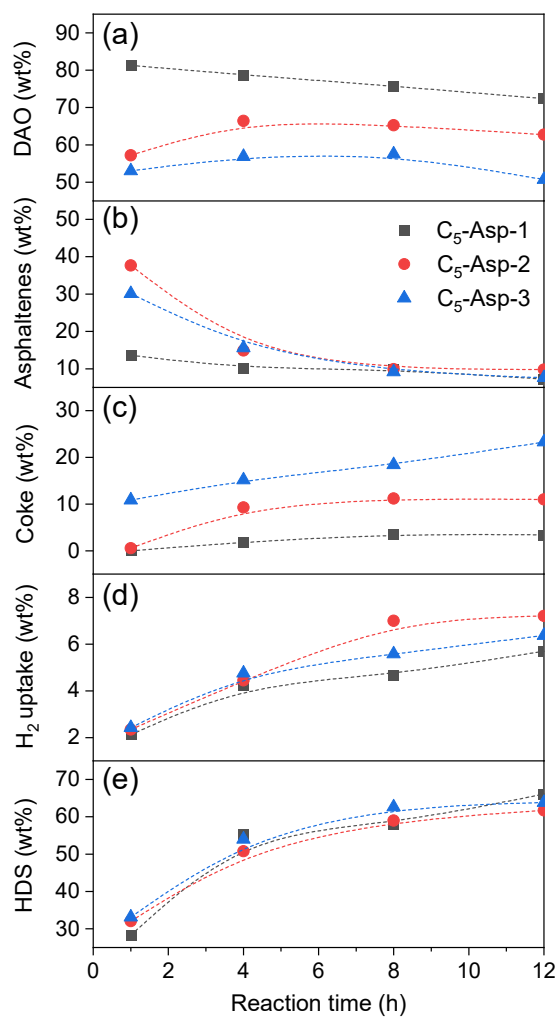
Figure 7. Yields for (**a**) DAO, (**b**) remaining asphaltenes, (**c**) coke, (**d**) H_2 consumption, and (**e**) hydrodesulfurization (HDS) during catalytic hydrocracking of asphaltene subfractions in the semi-batch system. Reaction conditions: T = 410 °C, P_{H2} = 110 bar, and 1000 wppm of Mo from Mo-octoate.
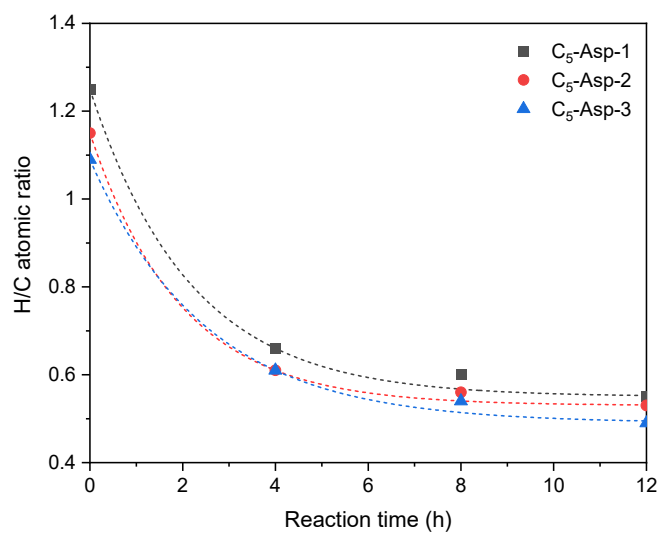
Figure 8. H/C atomic ratio of coke obtained from catalytic hydrocracking of asphaltene subfractions in the semi-batch system. Reaction conditions: T = 410 °C, P_{H2} = 110 bar, and 1000 wppm of Mo from Mo-octoate.

Figure 9 shows the XRD patterns of coke obtained from the catalytic hydrocracking of asphaltene subfractions. In our previous study [36], it was shown that the carbonaceous and condensation coke had a higher aggregation tendency to form hard graphitic coke. Hard graphitic coke is known to be the main cause of catalyst deactivation, assigned by a peak at 26° in the XRD pattern of coke [44]. The intensity of the graphite peak at 26° decreased in the following order: C_5-Asp-3 > C_5-Asp-2 > C_5-Asp-1. TG and DTG profiles of coke obtained from the catalytic hydrocracking of the asphaltene subfractions are also shown in Figure 9. TG/DTG analysis is applied to investigate the hardness of graphitic coke, where the type of coke is distinguished by the weight loss temperature in the range of 300–600 °C [45]. The decomposition temperature range of coke increased as the heaviness of asphaltene increased. The coke formed from C_5-Asp-1 showed two peaks at 380–410 °C while C_5-Asp-2 and C_5-Asp-3 fractions showed only one peak at 410–470 °C. The main peak temperature of coke decreased in the following order: C_5-Asp-3 > C_5-Asp-2 > C_5-Asp-1, which is well correlated with the H/C atomic ratio XRD results. These results support that more coke containing more hard graphitic coke is produced from the heavier asphaltenes during the catalytic hydrocracking.
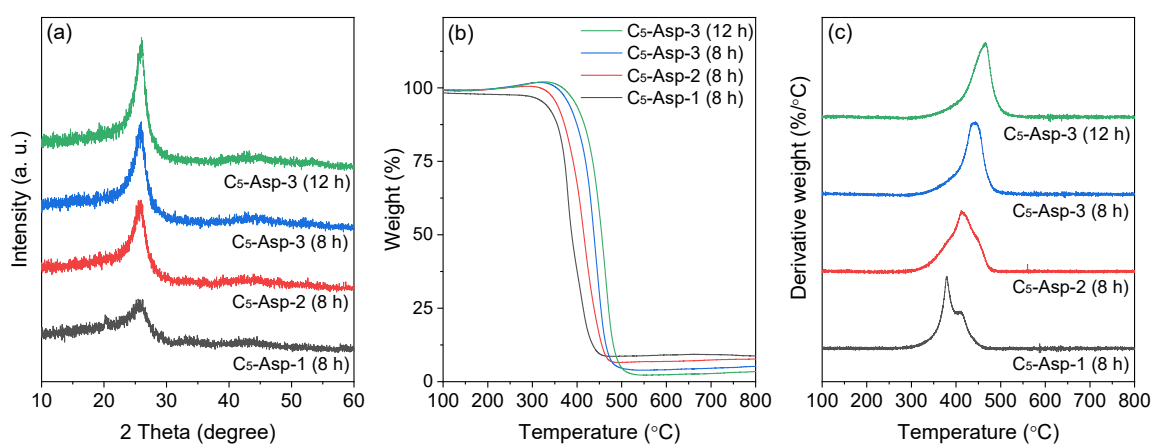
Figure 9. (**a**) XRD, (**b**) TG, and (**c**) DTG results of coke obtained from catalytic hydrocracking of asphaltene subfractions in the semi-batch system. Reaction conditions: T = 410 °C, P_{H2} = 110 bar, and 1000 wppm of Mo from Mo-octoate.

4. Conclusions

Catalyst and H_2 played an important role in the hydrocracking of C_5-asphaltenes. In the batch reaction system, the catalyst increased the asphaltene conversion into light liquid products and suppressed the formation of coke. The coke formation was suppressed at a low reaction temperature of 380 °C in batch reactor, but the reaction rate was too low. Light liquid products were formed from asphaltenes at the beginning of the hydrocracking reaction even at high temperatures, but the coke formation was then predominant as the reaction time went on due to the decrease in H_2 amount in the reactor. To solve these problems, H_2 was continuously supplied during the reaction using the semi-batch system. Sufficient supply of H_2 during the catalytic hydrocracking of asphaltenes improved the conversion of asphaltenes to resins and aromatics while inhibiting the coke formation. The lightest asphaltene fraction was easily cracked into light products by inhibiting the coke formation and it could prolong coke induction period of the heaviest fraction of the unfractionated asphaltenes during the catalytic hydrocracking. More coke containing more hard graphitic coke was produced from the heavier asphaltenes, which was the most problematic material in the heavy oil hydroconversion process.

Author Contributions: Conceptualization, N.T.N.; methodology, N.T.N., D.V.P., and P.W.S.; validation, K.H.K., S.P., and G.T.K.; formal analysis, N.T.N., N.K., and C.A.; investigation, N.T.N.; resources, N.T.N., K.H.K., and S.P.; writing—original draft preparation, N.T.N.; writing—review and editing, K.H.K. and S.P.; visualization, N.T.N., K.H.K., and S.P.; supervision, S.P. and G.T.K.; project administration, G.T.K. All authors have read and agreed to the published version of the manuscript.

Conflicts of Interest: The authors declare no conflict of interest.

References

1. Speight, J.G. New approaches to hydroprocessing. *Catal. Today* **2004**, *98*, 55–60. [CrossRef]
2. Rana, M.S.; Sámano, V.; Ancheyta, J.; Diaz, J.A.I. A review of recent advances on process technologies for upgrading of heavy oils and residua. *Fuel* **2007**, *86*, 1216–1231. [CrossRef]
3. Matsumura, A.; Kondo, T.; Sato, S.; Saito, I.; de Souza, W.F. Hydrocracking Brazilian Marlim vacuum residue with natural limonite. Part 1: Catalytic activity of natural limonite. *Fuel* **2005**, *84*, 411–416. [CrossRef]
4. Matsumura, A.; Sato, S.; Kondo, T.; Saito, I.; de Souza, W.F. Hydrocracking Brazilian Marlim vacuum residue with natural limonite. Part 2: Experimental cracking in a slurry-type continuous reactor. *Fuel* **2005**, *84*, 417–421. [CrossRef]
5. Gray, M.R.; McCaffrey, W.C. Role of chain reactions and olefin formation in cracking, hydroconversion, and coking of petroleum and bitumen fractions. *Energy Fuels* **2002**, *16*, 756–766. [CrossRef]
6. Du, H.; Liu, D.; Li, M.; Wu, P.; Yang, Y. Effects of the temperature and initial hydrogen pressure on the isomerization reaction in heavy oil slurry-phase hydrocracking. *Energy Fuels* **2015**, *29*, 626–633. [CrossRef]
7. Du, H.; Liu, N.; Liu, H.; Gao, P.; Lv, R.; Li, M.; Lou, B.; Yang, Y. Role of hydrogen pressure in slurry-phase hydrocracking of Venezuela heavy oil. *Energy Fuels* **2015**, *29*, 2104–2110. [CrossRef]
8. Mullins, O.C.; Sheu, E.Y.; Hammami, A.; Marshall, A.G. *Asphaltenes, Heavy Oils, and Petroleomics*; Springer: New York, NY, USA, 2010.
9. Ancheyta, J.; Trejo, F.; Rana, M.S. *Asphaltenes Chemical Transformation during Hydroprocessing of Heavy Oils*; CRC Press–Taylor & Francis Group: New York, NY, USA, 2009.
10. Christopher, J.; Sarpal, A.S.; Kapur, G.S. Chemical structure of bitumen-derived asphaltenes by nuclear magnetic resonance spectroscopy and X-ray diffractometry. *Fuel* **1996**, *75*, 999–1008. [CrossRef]
11. Absi-Halabi, M.; Stanislaus, A.; Trimm, D.L. Coke formation on catalysts during the hydroprocessing of heavy oils. *Appl. Catal.* **1991**, *72*, 193–215. [CrossRef]
12. Marchal, C.; Abdessalem, E.; Tayakout-Fayolle, M.; Uzio, D. Asphaltene diffusion and adsorption in modified NiMo alumina catalysts followed by ultraviolet (UV) spectroscopy. *Energy Fuels* **2010**, *24*, 4290–4300. [CrossRef]
13. Faus, F.M.; Grange, P.; Delmon, B. Influence of asphaltene deposition on catalytic activity of cobalt molybdenum on alumina catalysts. *Appl. Catal.* **1984**, *11*, 281–293. [CrossRef]
14. Ancheyta, J.; Centeno, G.; Trejo, F.; Marroquin, G. Changes in asphaltene properties during hydrotreating of heavy crudes. *Energy Fuels* **2003**, *17*, 1233–1238. [CrossRef]
15. Trejo, F.; Ancheyta, J. Kinetics of asphaltenes conversion during hydrotreating of Maya crude. *Catal. Today* **2005**, *109*, 99–103. [CrossRef]
16. Trejo, F.; Ancheyta, J.; Centeno, G.; Marroquin, G. Effect of hydrotreating conditions on Maya asphaltenes composition and structural parameters. *Catal. Today* **2005**, *109*, 178–184. [CrossRef]
17. Ancheyta, J.; Centeno, G.; Trejo, F. Asphaltene characterization as function of time on-stream during hydroprocessing of Maya crude. *Catal. Today* **2005**, *109*, 162–166. [CrossRef]
18. Goncalve, M.L.A.; Ribeiro, D.A.; Teixeira, A.M.R.F.; Teixeira, M.A.G. Influence of asphaltenes on coke formation during the thermal cracking of different Brazilian distillation residues. *Fuel* **2007**, *86*, 619–623. [CrossRef]
19. Wang, J.; Anthony, E.J. A study of thermal-cracking behavier of asphaltenes. *Chem. Eng. Sci.* **2003**, *58*, 157–162. [CrossRef]
20. Martinez, M.T.; Benito, A.M.; Callejas, M.A. Thermal cracking of coal residues: Kinetics of asphaltene decomposition. *Fuel* **1997**, *76*, 871–877. [CrossRef]
21. Rahmani, S.; Gray, M.R. Dependence of molecular kinetics of asphaltene cracking on chemical composition. *Pet. Sci. Technol.* **2007**, *25*, 141–152. [CrossRef]
22. Nguyen, N.T.; Park, S.; Jung, J.; Cho, J.; Lee, C.W.; Park, Y.-K. Comparative reactivity between thermal and catalytic hydrocracking of vacuum residue: Effect of asphaltenes. *J. Ind. Eng. Chem.* **2018**, *61*, 32–38. [CrossRef]

23. Akmaz, S.; Gurkaynak, M.A.; Yasar, M. The effect of temperature on the molecular structure of Raman asphaltenes during pyrolysis. *J. Anal. Appl. Pyrolysis* **2012**, *96*, 139–145. [CrossRef]

24. Zhao, Y.; Wei, F.; Yu, Y. Effects of reaction time and temperature on carbonization in asphaltene pyrolysis. *J. Petro. Sci. Eng.* **2010**, *74*, 20–25. [CrossRef]

25. Douda, J.; Alvarez, R.; Bolanos, J.N. Characterization of Maya asphaltene and maltene by mean of pyrolysis application. *Energy Fuels* **2008**, *22*, 2619–2628. [CrossRef]

26. Zhang, C.; Lee, C.W.; Keogh, R.A.; Demirel, B.; Davis, B.H. Thermal and catalytic conversion of asphaltenes. *Fuel* **2001**, *80*, 1131–1146. [CrossRef]

27. Yasar, M.; Trauth, D.M.; Klein, M.T. Asphaltene and resid pyrolysis. 2. The effect of reaction environment on pathways and selectivities. *Energy Fuels* **2001**, *15*, 504–509. [CrossRef]

28. Rezaei, H.; Liu, X.; Ardakani, S.J.; Smith, K.J.; Bricker, M. A study of Cold Lake vacuum residue hydroconversion in batch and semi-batch reactors using unsupported MoS_2 catalysts. *Catal. Today* **2010**, *150*, 244–254. [CrossRef]

29. Otiz-moreno, H.; Ramirez, J.; Sanchez-minero, F.; Cuevas, R.; Ancheyta, J. Hydrocracking of Maya crude oil in a slurry-phase batch reactor. II. Effect of catalyst load. *Fuel* **2014**, *130*, 263–272. [CrossRef]

30. Martinez-grimaldo, H.; Otiz-moreno, H.; Sanchez-minero, F.; Ramirez, J.; Cuevas-garcia, R.; Ancheyta, J. Hydrocracking of Maya crude oil in a slurry-phase batch reactor. II. Effect of reaction temperature. *Catal. Today* **2014**, *130*, 269–272. [CrossRef]

31. Panariti, N.; Del Bianco, A.; Del Piero, G.; Marchionna, M. Petroleum residue upgrading with dispersed catalyst: Part 1. Catalysts activity and selectivity. *Appl. Catal. A Gener.* **2000**, *204*, 203–213. [CrossRef]

32. Kang, K.H.; Nguyen, N.T.; Seo, P.W.; Seo, H.; Kim, G.T.; Kang, N.; Lee, C.W.; Han, S.J.; Chung, M.-C.; Park, S. Slurry-phase hydrocracking of heavy oil over Mo precursors: Effect of triphenylphosphine ligands. *J. Catal.* **2020**, *384*, 106–121. [CrossRef]

33. Miki, Y.; Yamadaya, S.; Oba, M.; Sugimoto, Y. Role of catalyst in hydrocracking of heavy oil. *J. Catal.* **1983**, *83*, 371–383. [CrossRef]

34. Trejo, F.; Centeno, G.; Ancheyta, J. Precipitation, fractionation and characterization of asphaltenes from heavy and light crude oils. *Fuel* **2004**, *83*, 2169–2175. [CrossRef]

35. Kaminski, T.J.; Fogler, H.S.; Wolf, N.; Wattana, P.; Mairal, A. Classification of asphaltenes via fractionation and the effect of heteroatom content on dissolution kinetics. *Energy Fuels* **2000**, *14*, 25–30. [CrossRef]

36. Nguyen, N.T.; Kang, K.H.; Lee, C.W.; Kim, G.T.; Park, S.; Park, Y.-K. Structure comparison of asphaltene aggregates from hydrothermal and catalytic hydrothermal cracking of C_5-isolated asphaltene. *Fuel* **2019**, *235*, 677–686. [CrossRef]

37. Bartholdy, J.; Andersen, S.I. Changes in asphaltene stability during hydrotreating. *Energy Fuels* **2000**, *14*, 52–55. [CrossRef]

38. Buch, L.; Groenzin, H.; Buenrostro-Gonzalez, E.; Andersen, S.I.; Lira-Galeana, C.; Mullins, O.C. Molecular size of asphaltene fractions obtained from residuum hydrotreatment. *Fuel* **2003**, *82*, 1075–1084. [CrossRef]

39. Zou, R.; Liu, L.; Yen, T.F.; Chilingarian, G.V. *Asphaltenes and Asphalts, Vol 1*; Elsevier Science B.V: New York, NY, USA, 1994; p. 339.

40. Callejas, M.A.; Martínez, M.T. Hydroprocessing of a Maya residue. 1. Intrinsic kinetics of asphaltene removal reactions. *Energy Fuels* **2000**, *14*, 1304–1308. [CrossRef]

41. Seki, H.; Kumata, F. Structural change of petroleum asphaltenes and resins by hydrodemetallization. *Energy Fuels* **2000**, *14*, 980–985. [CrossRef]

42. Li, C.; Han, Y.; Yang, T.; Deng, W. Preliminary study on the influence of catalyst dosage on coke formation of heavy oil slurry-bed hydrocracking. *Fuel* **2020**, *270*, 117489. [CrossRef]

43. Rezaei, H.; Smith, K.J. Catalyst deactivation in slurry-phase residue hydroconversion. *Energy Fuels* **2013**, *27*, 6087–6097. [CrossRef]

44. Mullins, O.C. The modified Yen model. *Energy Fuels* **2010**, *24*, 2179–2207. [CrossRef]

45. Han, S.J.; Kim, S.K.; Hwang, A.; Kim, S.; Hong, D.-Y.; Kwak, G.; Jun, K.-W.; Kim, Y.T. Non-oxidative dehydroaromatization of methane over Mo/H-ZSM-5 catalysts: A detailed analysis of the reaction regeneration cycle. *Appl. Catal. B* **2019**, *241*, 305–318. [CrossRef]